Pediatr Nephrol (2010) 25:1245–1253
DOI 10.1007/s00467-010-1493-2

ORIGINAL ARTICLE

Heat shock protein 70 induction and its urinary excretion in a model of acetaminophen nephrotoxicity

Sara M. Molinas · Marina Rosso · Nahuel Z. Wayllace · Melina A. Pagotto · Gerardo B. Pisani · Liliana A. Monasterolo · Laura Trumper

Received: 15 September 2009 / Revised: 12 January 2010 / Accepted: 15 January 2010 / Published online: 30 March 2010
© IPNA 2010

Abstract Acetaminophen (APAP) is an analgesic–antipyretic drug widely used in children. In the present study, we used an in vivo model of APAP-induced nephrotoxicity in male Wistar rats. We analyzed whether toxic doses of APAP could induce heat shock protein 70 (HSP70) in the kidney and whether HSP70 could be detected in urine. Renal function and histological evaluation of the kidneys were performed at different times after APAP administration (1,000 mg/kg body weight i.p.). Cellular injury was assessed by Triton X-100 solubilization of Na^+/K^+ ATPase. Renal and hepatic glutathione levels were also measured. Urinary N-acetyl-β-D glucosaminidase (NAG) excretion increased 4 h after intoxication. At this time, urea and creatinine were at control levels and a slight degree of histological alteration was detected. Kidney microscopic evaluation, Na^+/K^+ ATPase solubility, creatinine, and urea levels and NAG excretion did not differ from those of controls 48 h after APAP administration. HSP70 was detected in urine obtained from 4 to 24 h after APAP administration. HSP70 abundance in renal cortex was increased at early time points and 48 h after APAP administration. Urinary HSP70 excretion would be a marker of its renal induction combined with the loss of tubule integrity. NAG would be a suitable early biomarker of APAP-induced nephrotoxicity.

Keywords Kidney · Acetaminophen-induced nephrotoxicity · HSP70 · Glutathione · Na^+ · K^+ ATPase · N-acetyl-β-D glucosaminidase

S. M. Molinas · M. A. Pagotto · L. A. Monasterolo
Consejo Nacional de Investigaciones Científicas y Técnicas (CONICET),
Rosario, Argentina

M. Rosso · N. Z. Wayllace
Farmacología, Facultad de Ciencias Bioquímicas y Farmacéuticas,
Universidad Nacional de Rosario,
Rosario, República Argentina

G. B. Pisani
Morfología, Facultad de Ciencias Bioquímicas y Farmacéuticas,
Universidad Nacional de Rosario,
Rosario, Argentina

L. Trumper
Consejo de Investigaciones de la Universidad Nacional de Rosario (CIUNR),
Rosario, Argentina

L. Trumper (✉)
Farmacología, Facultad de Ciencias Bioquímicas y Farmacéuticas,
Suipacha 531-2000,
Rosario, Argentina
e-mail: ltrumper@fbioyf.unr.edu.ar

Introduction

Acetaminophen (APAP) is one of the most widely prescribed analgesic and antipyretic drugs in young children. Although it is considered safe in therapeutic doses, in overdose situations it produced hepatic necrosis and renal failure in both human and experimental animals [1–3]. APAP overdose produced acute proximal tubular necrosis in male Fischer rats [4–6] and in the CD-1 mouse [7]. Renal damage can occur even in the absence of liver injury [2, 8].

We have previously reported the development of APAP-induced acute renal failure after the administration of a toxic dose of APAP to male Wistar rats. Sixteen hours after dosing, impairment of renal hemodynamic and tubular functions was observed. Renal function

recovered 48 h after APAP administration [9]. We also reported an increment in the Triton X-100 extractability of Na^+/K^+ ATPase in freshly isolated cortical cell suspensions incubated with APAP [10]. Triton X-100 extractability fractionates the cellular pool of Na^+/K^+ ATPase into an insoluble pellet (cytoskeleton-associated) and a soluble supernatant [11]. Detachment of Na^+/K^+ ATPase from its cytoskeletal anchorage to the basolateral membrane has been used as a marker of cellular integrity [11–13].

The 70-kDa family of heat shock proteins (HSP70) plays a central role in cellular protection [14]. HSP70 is the major inducible molecular chaperone found in mammalian cells [15]. In the kidney, the 70-kDa HSP production localizes primarily in renal tubular cells [16]. HSP70 has been associated with cytoprotection in response to several injuries, including oxidative stress [17], ischemia [18, 19], and nephrotoxicity [20, 21]. In renal epithelial cells exposed to nephrotoxic cysteine conjugates, it was reported that changes in protein structure or conformation triggers the increase in HSP70 mRNA [22]. Cytoprotective effects of HSP70 rely on its ability to bind non-native proteins and chaperone their refolding or elimination [23]. Heat shock proteins (HSP) have been involved in the restitution of the cytoskeletal anchorage of Na^+/K^+ ATPase [24, 25]. Urinary HSP70 excretion has been observed in pediatric allograft recipients and in an experimental model of renal ischemia [26].

Acetaminophen toxicity results from its metabolism to the reactive metabolite N-acetyl-*p*-benzoquinone imine (NAPQI) by cytochrome P450. At low doses, NAPQI is detoxified by conjugation with glutathione (GSH). Following toxic doses, GSH becomes depleted and NAPQI binds to protein targets [27]. The mechanism of hepatic APAP toxicity is well described, but it is less clearly understood in the kidney. In rats, possible renal mechanisms include the cytochrome pathway and deacetylation to p-aminophenol [28]; however, in the CD-1 mouse it has been shown that deacetylation is not a prerequisite [7]. We have shown previously the contribution of GSH-derived APAP metabolites formed in the liver in the development of APAP-induced nephrotoxicity [29].

In the present study we used an in vivo model of APAP-induced nephrotoxicity. We studied the time course changes in renal function and histological damage after APAP administration. Cellular injury was also assessed by solubilization of Na^+/K^+ ATPase. We seek to analyze whether toxic doses of APAP could induce HSP70 in the renal cortical tissue and its urinary excretion. Renal and hepatic GSH levels were also measured as an indirect index of the production of APAP toxic metabolites.

Materials and methods

Animals and treatments

Male Wistar rats (3 months; 250–350 g body weight) were used. Animals were housed in rooms with controlled temperature (21–23°C), and regular light cycles (12 h). They were allowed free access to a standard diet and tap water until used. Experiments were performed in accordance with the guide for the care and use of laboratory animals promulgated by the National Institute of Health (National Centre for Research Resources, Bethesda, MD, USA) and approved by our institutional ethics committee. Rats were fasted for 16 h (5 p.m. to 9 a.m.) before the experiments and were allowed free access to water. Animals received a single dose of APAP (Sigma Chemical Company, St. Louis, MO, USA) of 1,000 mg/kg body weight i.p. at 5 ml/kg in propylene glycol:saline (1:1). A group of animals received the corresponding volume of APAP vehicle (C). The dose and the time points studied were chosen based on our previous results [9].

Effect of APAP on renal and hepatic function

After APAP administration, rats were placed on metabolic cages for urine collection. Four ($APAP_4$), 6 ($APAP_6$), 16 ($APAP_{16}$), 24 ($APAP_{24}$), and 48 h ($APAP_{48}$) after APAP administration, rats were anesthetized with sodium thiopental (70 mg/kg body weight i.p.). A blood sample was obtained from the abdominal cava vein for creatinine, urea, and alanine aminotransferase (ALT) measurement. Urine volume was estimated gravimetrically.

Histopathological studies

Excised kidneys were processed for light microscopic observation, according to standard procedures. Briefly, the tissue was fixed in 10% formaldehyde, embedded in paraffin and sectioned (5 μm). The sections were stained with hematoxylin and eosin (H&E) or periodic acid-Schiff (PAS) and examined under a light microscope.

Effect of APAP on Na^+/K^+ ATPase solubility, and on cortical HSP70 and GSH content

A group of animals received the toxic dose of APAP and were sacrificed 6, 16, and 48 h after APAP administration. Rats were anesthetized as described previously, and kidneys were promptly removed. Kidneys were decapsulated in chilled isotonic solution and the cortex was dissected out. Cortical tissues were homogenized in chilled extraction buffer [13] containing 60 mM piperazine-*N,N′*-bis(2-

ethanesulfonic acid) (PIPES), 1 mM ethylene glycol-bis(β-aminoethyl ether)-*N,N,N′,N′*-tetraacetic acid (EGTA), 1 mM EDTA, 100 mM NaCl, pH 6.9 with 0.1% Triton X-100, 0.5 mM phenylmethyl sulfonyl fluoride, and 0.1 mM dithiothreitol in a motor-driven Teflon-glass Potter homogenizer. The homogenates were centrifuged at 680 g for 10 min at 4° to remove large cellular fragments and nuclei. The supernatants were saved at −70° for HSP70 immunodetection. In a set of experiments, the supernatants were immediately centrifuged at 35,000 g for 14 min at 4° to separate the Triton X-100-soluble protein fraction (S) from the insoluble cytoskeletal fraction (I). The detergent extractable supernatant was carefully removed and the pellet was resuspended in the same volume of extraction buffer. All samples were saved at −70° until further immunodetection of Na^+/K^+ ATPase. Samples of cortical homogenates were also saved for HSP70 immunodetection.

We also performed a set of experiments where livers were removed and homogenized 4, 16, 24 or 48 h after APAP administration for immunodetection of HSP70.

For glutathione assays, nonprotein sulfhydryls were measured in livers and in renal cortical homogenates. Homogenates were prepared in cold 5% trichloroacetic acid in 0.01 M HCl and glutathione was measured as described previously [30]. Results were expressed as micromoles per gram of wet tissue.

Gel electrophoresis and immunoblotting

To analyze Na^+/K^+ ATPase solubility, samples from Triton X-100 soluble and insoluble fractions (10 μg protein each) were run on sodium dodecyl sulfate 8% polyacrylamide gels (SDS-PAGE; Bio-Rad Mini Protean 3, Hercules, CA, USA) [31]. For each gel, an identical gel was run in parallel and subjected to Coomassie staining to ensure identical loading. The amount of protein was chosen after the linearity of detection had been verified. Samples were boiled 3 min in the presence of 5% 2-mercaptoethanol and 1% SDS. Five microliters of prestained molecular weight standards were also loaded onto the gel. The separated proteins were transferred onto nitrocellulose membranes (BioRad) in Tris-glycine transfer buffer with 20% methanol in a mini-blotter (Sigma–Aldrich). Uniform blotting across the gel was verified by Coomassie brilliant blue staining of the post blot gel. Nitrocellulose membranes were incubated for 1 h at room temperature with 5% (wt/vol) non-fat dry milk in phosphate buffered saline (PBS), followed by a 1-h (room temperature) incubation with a goat polyclonal antibody to the rabbit kidney Na^+/K^+ ATPase α subunit (1:3,000 dilution; Calbiochem-Novabiochem Corporation, La Jolla, CA, USA). After washing, membranes were incubated for 1 h with alkaline phosphatase-conjugated anti-goat antibody (1:3,000 dilution, Santa Cruz Biotechnologies, Santa Cruz, CA, USA). After washing, bound alkaline phosphatase was detected with 5-bromo-4-chloro-3-indolyl phosphate/nitroblue tetrazolium (Promega, Madison, WI, USA).

In renal cortical homogenates (10 μg protein), in urine samples (20 μg protein), and in liver homogenates (10 μg protein) HSP70 levels were detected by SDS-PAGE and Western blotting as described above. Non-specific background was blocked by incubating the membranes with 5% non-fat dry milk in Tris-buffered saline with 0.05% Tween 20. Membranes were then incubated overnight with the anti-HSP70 goat polyclonal (1:1,000 dilution, K-20; Santa Cruz Biotechnologies). Detection was achieved as described above with an alkaline phosphatase-conjugated anti-goat antibody. Membranes of cortical homogenates

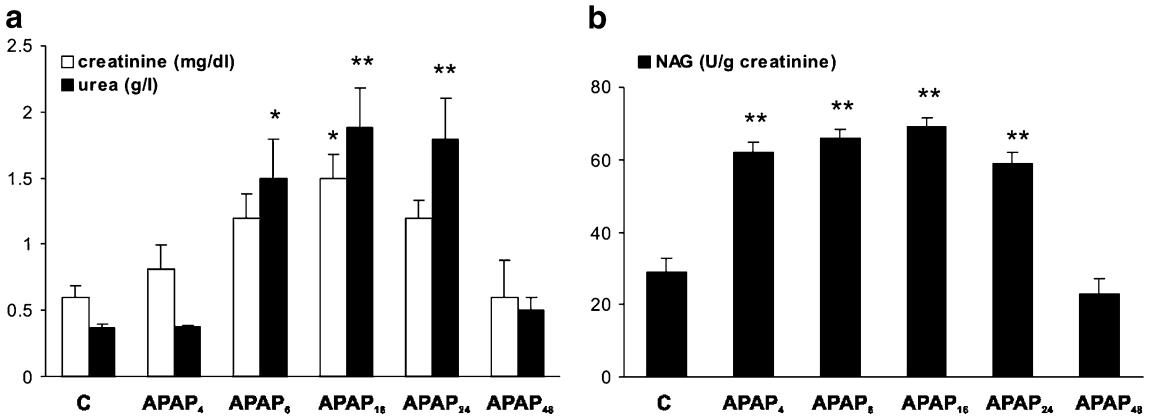

Fig. 1 Effects of acetaminophen (APAP) on renal function after the administration of a single dose of 1,000 mg/kg body weight i.p. **a** Plasma creatinine and urea levels were measured in controls (n=6) and 4 h ($APAP_4$, n=5), 6 h ($APAP_6$, n=6), 16 h ($APAP_{16}$, n=6), 24 h ($APAP_{24}$, n=6), and 48 h ($APAP_{48}$, n=4) after APAP administration. **b** Urinary N-acetyl-β-D glucosaminidase (NAG) was measured in urine from rats after the same times as described in **a**. Data are mean ± SE. *p<0.05 compared with control, **p<0.01 compared with control

were stripped and reprobed with a rabbit polyclonal anti-actin antibody (1:600 dilution; Santa Cruz Biotechnologies) and an alkaline phosphatase-conjugated anti-rabbit antibody (1:3,000 dilution; Santa Cruz Biotechnologies).

Blots were digitized using a desktop computer Scanner (HP II Scan Jet). Densitometry analyses of membranes were performed on a PC computer using the Adobe PhotoShop (6.0) computer program.

Analytical methods

Plasma creatinine was determined by a kinetic alkaline picrate method (Jaffé reaction) with a commercial kit (Wiener Laboratories, Rosario, Argentina). Urea and plasma alanine aminotransferase were measured with commercial kits (Wiener Laboratories, Rosario, Argentina). Urinary NAG was measured following the method of Hosseini et al. [32]. Proteins were measured with Coomassie brilliant blue G250 [33] using bovine serum albumin as standard.

Statistical analysis

Results are expressed as mean and standard error of the mean (SE). Data were analyzed using the one-way analysis of variance followed by Bonferroni contrasts, using a computer program (Graphpad Instat, version 1.15). The 0.05 level of probability was used as the criterion for significance in all cases.

Results

Effect of APAP on renal function and cellular injury

Renal function was evaluated by the plasma creatinine and urea levels. Plasma creatinine was significantly increased 16 h after the administration of a toxic dose of APAP. Urea levels were elevated 6, 16, and 24 h after APAP administration. Both creatinine and urea levels returned to control values 48 h after APAP administration (Fig. 1a). Tubular injury was evaluated by the urinary NAG excretion. As shown (Fig. 1b), urinary NAG excretion was significantly increased 4 h after APAP intoxication. Urine flow rate decreased 4 h after APAP administration and returned to control values after 48 h ($C = 4.50 \pm 0.4$; $APAP_4 = 1.26 \pm 0.5$*, $APAP_6 = 1.30 \pm 0.5$*; $APAP_{16} = 1.90 \pm 0.5$*; $APAP_{24} = 2.1 \pm 0.5$*; $APAP_{48} = 4.1 \pm 0.5$ μl/min/100gb.wt., *$p<0.05$ vs C). Total urinary protein excretion was significantly increased 16 and 24 h after APAP administration ($C = 0.7 \pm 0.2$; $APAP_4 = 1.5 \pm 0.2$, $APAP_6 = 1.2 \pm 0.1$; $APAP_{16} = 2.16 \pm 0.2$*; $APAP_{24} = 1.9 \pm 0.3$* ; $APAP_{48} = 0.8 \pm 0.2$ mg/ml, *$p<0.05$ vs C).

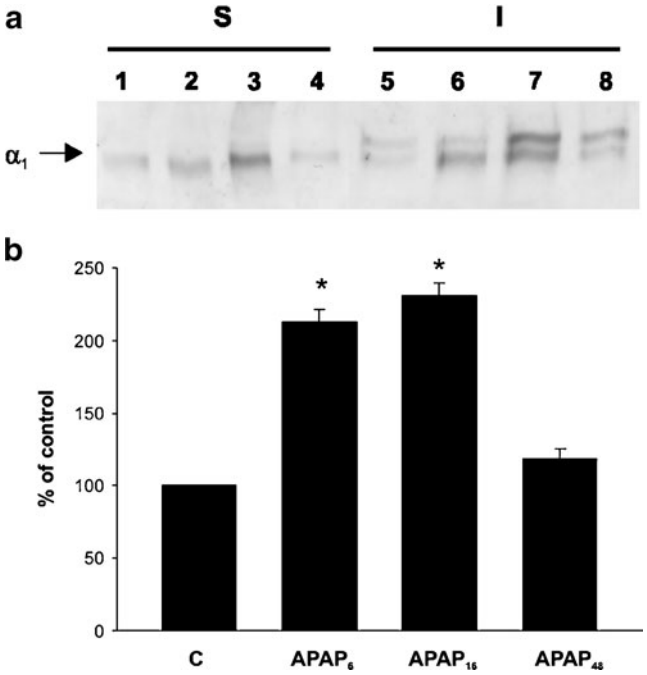

Fig. 2 Na^+/K^+ ATPase abundance in Triton soluble (S) and insoluble fractions (I) of renal cortex. **a** Representative Western blot showing an immunodetectable α_1 Na^+/K^+ ATPase subunit. Lanes 1 and 5: C; lanes 2 and 6: $APAP_6$; lanes 3 and 7 $APAP_{16}$, lanes 4 and 8: $APAP_{48}$. **b** α_1 subunit abundance in arbitrary densitometry units expressed as (S/S+I). The magnitude of the signal is given as a percentage of control samples. Each result is the mean ± SE of 4–6 experiments. *$p<0.05$ compared with control

Cellular injury was assessed by the solubilization of Na^+/K^+ ATPase. Protein levels of the Na^+/K^+ ATPase α_1 subunit were evaluated by Western blot analysis in the Triton X-100 soluble and insoluble fractions from cortical homogenates. The ratio between the abundance of Na^+/K^+ ATPase α_1 subunit in the soluble fraction and its total abundance, measured as the sum of the abundance in the soluble and the insoluble fractions (S/S+I), was increased in the groups studied 6 h and 16 h after APAP administration. Forty-eight hours after APAP intoxication the ratio S/S+I did not differ from that observed in the control group (Fig. 2).

Morphological alterations after APAP treatment were evaluated by light microscopy. Figure 3a–j shows sections stained with H&E (×200). Figure 3k–o shows sections stained with PAS (×400). Four hours after APAP administration, a slight vacuolization and desquamation of tubular cells (Fig. 3b), and some areas characterized by a

Fig. 3 Effects of APAP on tissue damage. Histological characteristics ▶ were analyzed by light microscopy in tissue sections from kidneys of control rats (**a**, **f**, **k**) and 4 h (**b**, **g**, **l**); 16 h (**c**, **h**, **m**); 24 h (**d**, **i**, **n**), and 48 h (**e**, **j**, **o**) after APAP administration. **a–j** show sections stained with H&E (×200). **k–o** show sections stained with PAS (×400). *Asterisks* show desquamated tubular cells, *unfilled arrowheads* show vacuolization of tubular cells, *filled arrowheads* show tubular casts, and *arrows* show areas of diminished brush border

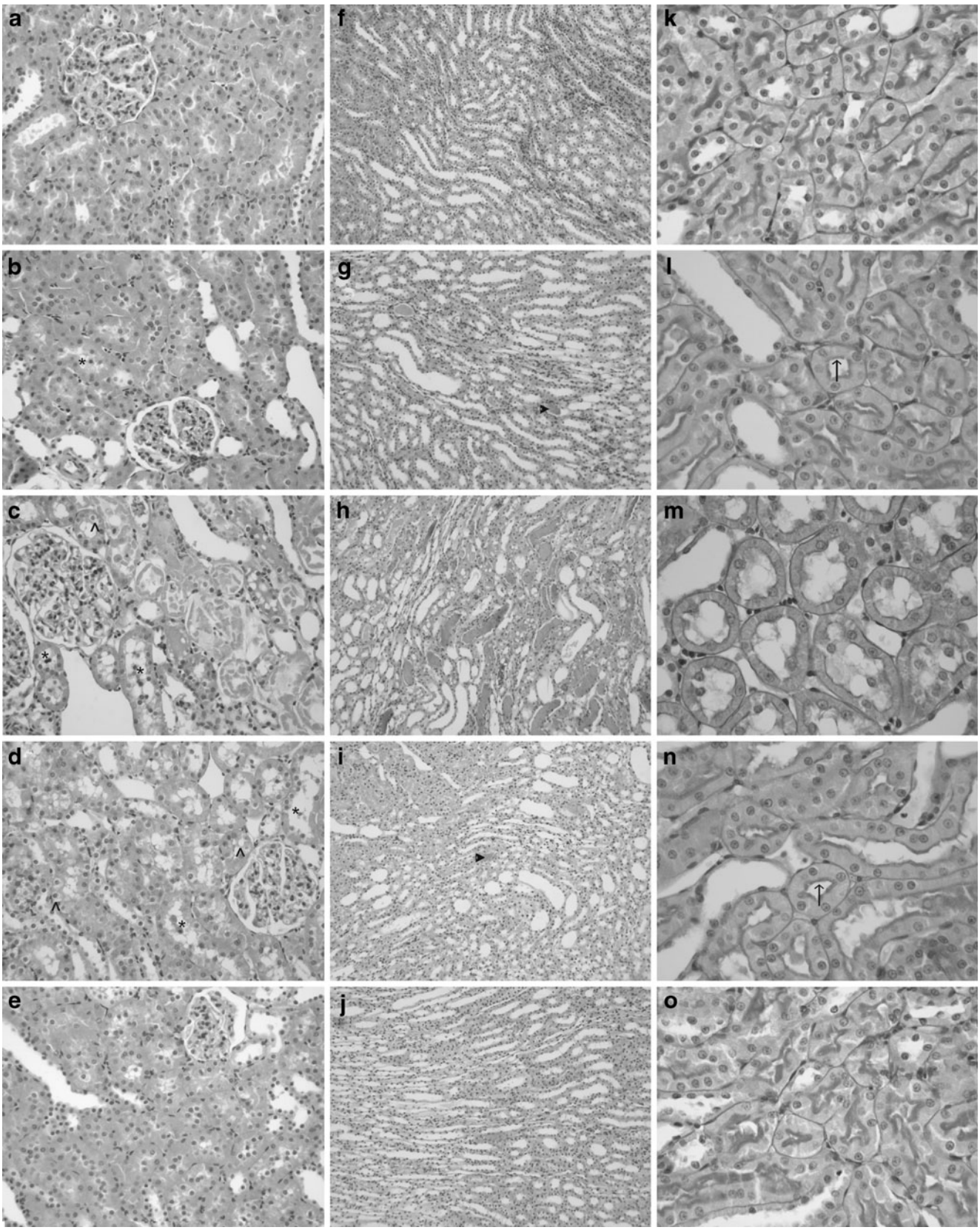
a
f
k
b
g
l
c
h
m
d
i
n
e
j
o

diminished brush border and lumen dilatation (Fig. 3g, l) were observed. Kidneys studied 16 h after APAP administration showed severe cortical necrosis, lumen dilatation, vacuolization of tubular cell cytoplasm, abundant tubular casts, some of them with cellular detritus, and a marked diminution of the brush border (Fig. 3c, h, m). Twenty-four hours after, some tubular vacuoles, cellular desquamation, lumen dilatation, and tubular casts were observed (Fig. 3d, i). At this time a marked improvement of the tubular brush border was detected, although there were some areas of diminished brush border (Fig. 3n). Forty-eight hours after APAP administration, the kidneys presented preserved tubular structure (Fig. 3o). Only minor signs of vascular congestion were observed in $APAP_4$ and $APAP_{24}$, while this was more evident in the $APAP_{16}$ group. Glomeruli were preserved at all the times studied.

Effect of APAP on liver function

Changes in plasma ALT activity were examined as an index of liver damage. ALT was significantly elevated 4, 6, 16, and 24 h after APAP administration, returning to control values after 48 h ($C = 31 \pm 4$, $APAP_4 = 150 \pm 10$**, $APAP_6 = 185 \pm 12$**, $APAP_{16} = 180 \pm 15$**, $APAP_{24} = 200 \pm 18$** , $APAP_{48} = 32 \pm 5$ IU/L, **$p<0.01$ compared with C).

Effect of APAP on renal and liver glutathione content

Renal cortical glutathione levels were significantly decreased 16 h after APAP treatment and returned to control values after 48 h of APAP administration. Liver glutathione levels were decreased 6 h after APAP administration. At 48 h, liver glutathione levels were higher than control values (Table 1). Similar results were observed previously in our laboratory [9].

HSP70 induction in cortical homogenates and its urinary excretion

HSP70 was constitutively expressed in renal cortex from control rats. HSP70 levels were increased in cortical tissue obtained from rats 6, 16, and 48 h after APAP administration (Fig. 4).

In urine from control rats there was no detectable HSP70 excretion. In the $APAP_4$ group HSP70 was detected in urine, and the highest levels were observed 16 h after APAP administration. This is the time when the maximal deterioration of renal function and tissue damage was observed. After 48 h of APAP intoxication, no HSP70 was detected in urine (Fig. 5).

Effect of APAP on liver HSP70 content

As it has been suggested that covalent binding of NAPQI to hepatic macromolecules leads to liver injury and to HSP induction [34, 35] we studied the effects of APAP on hepatic HSP70 induction in our experimental model. Our aim was to clarify the source of urinary HSP70, so we analyzed hepatic HSP70 levels 4, 16, 24, and 48 h after APAP administration. APAP promoted no changes in hepatic HSP70 content (not shown), suggesting that liver would not be the source of the HSP70 that appears in urine.

Discussion

Acetaminophen is an analgesic–antipyretic drug widely prescribed in the pediatric population. In an overdose

Table 1 Time course changes in renal cortical and hepatic GSH content (μmol/g wet tissue) after a single dose of APAP (1,000 mg/kg body weight i.p.)

Time (h)	Renal cortex	Liver
Control (n=5)	1.8±0.1	3.1±0.2
6 (n=6)	1.1±0.2	1.2±0.1*
16 (n=6)	0.7±0.2**	1.9±0.3
48 (n=4)	2.1±0.2	5.5±0.9*

*$p<0.05$ compared with controls; **$p<0.01$ compared with controls

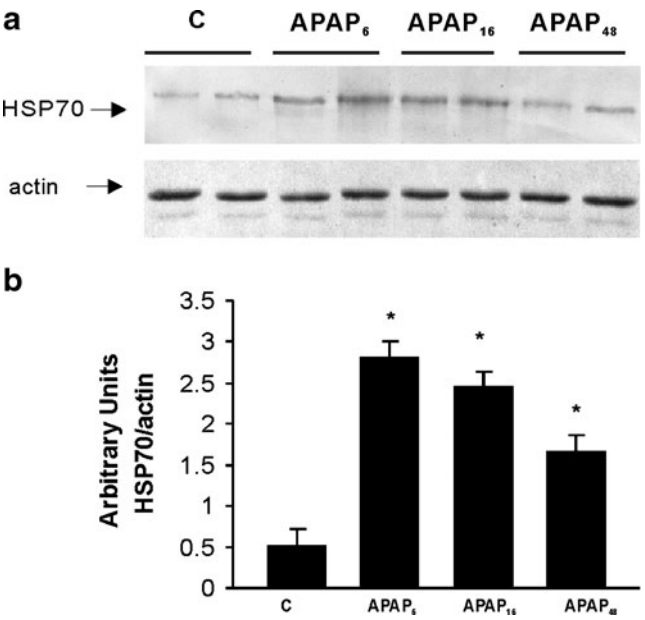

Fig. 4 Time course of changes in HSP70 abundance in cortical homogenates after APAP administration. **a** Representative immunoblot showing HSP70 detection in C, $APAP_6$, $APAP_{16}$, and $APAP_{48}$ cortical homogenates. Membranes were stripped and reprobed for actin. **b** Ratio between HSP70 and actin abundance in arbitrary densitometry units. Each result is the mean ± SE of six experiments. *$p<0.05$ compared with control

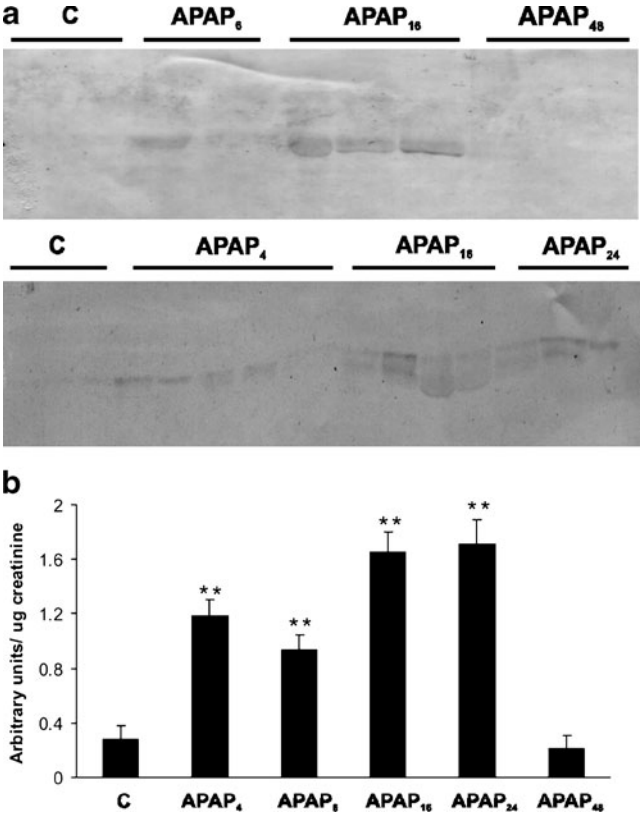

Fig. 5 Immunodetection of HSP70 in urine obtained from C rats and 4, 6, 16, 24, and 48 h after APAP administration. **a** Representative immunoblot showing HSP70 detection in urine from C, $APAP_4$ $APAP_6$, $APAP_{16}$, $APAP_{24}$, and $APAP_{48}$ rats. **b** Urinary HSP70 abundance in arbitrary densitometry units standardized to urinary creatinine. Each result is the mean ± SE of six experiments. $^{**}p<0.01$ compared with control

situation, it can produce hepatic and renal damage. In the present work we used an experimental model of APAP-induced acute nephrotoxicity. Plasma creatinine levels were increased 16 h after APAP intoxication, while urea levels increased after 6 h. Proteinuria was observed 16 and 24 h after APAP administration.

Urinary NAG increased 4 h after intoxication. It is noticeable that this occurs at a time when creatinine and urea are still within the control range. There are no specific early symptoms or signs of APAP poisoning. Patients with plasma APAP concentrations greater than 200 μg/ml 4 h after ingestion are considered severely poisoned [36] and prognosis depends on the early detection and implementation of therapeutics. Our present results suggest that urinary NAG would be a suitable early biomarker of APAP-induced nephrotoxicity.

Some evidence of histological damage was observed 4 h after APAP administration. Severe tubular necrosis, loss of the brush border, lumen dilatation, cellular desquamation, and intratubular cast formation were observed after 16 h. Less evidence of histological damage was observed 24 h after APAP administration. After 48 h, the kidney recovers its normal structure. No evidence of glomerular injury was observed at any of the times studied.

An increase in the abundance of Na^+/K^+ ATPase in the Triton X-100 soluble fractions 6 h and 16 h after APAP administration was observed. Forty-eight hours after APAP administration, the abundance of Na^+/K^+ ATPase in the soluble fraction did not differ from that observed in controls.

Taken together, these results suggest the loss of tubular cell integrity during the early stages of APAP-induced nephrotoxicity, and its restoration 48 h after APAP administration. These results are in agreement with our previous report of the reversibility of the APAP-induced impairment of renal function [9].

Liver function, assessed by the ALT levels, also returns to control values 48 h after APAP administration. GSH levels were measured as an indirect index of the production of APAP-toxic metabolites. Hepatic GSH content was decreased by APAP and values were restored and even higher than in control livers 48 h after APAP administration. Hepatic toxicity of APAP is known to be dependent on GSH depletion, and covalent binding of NAPQI to hepatic macromolecules. APAP metabolites form adducts with certain proteins [37] and this could trigger HSP70 induction [38]. The mechanism of renal toxicity is less clear. GSH content of the renal cortex was decreased only in the $APAP_6$ group. Six, 16, and 48 h after APAP administration HSP70 increased in cortical renal tissue. These results suggest that the adduction of NAPQI to renal proteins would not be the only mechanism of HSP induction in the kidney. In our experimental model, although we observed liver damage and hepatic GSH depletion, no hepatic induction of HSP70 was observed. However, the liver of APAP-treated mice has shown increased levels of HSP70 [34]. A likely explanation of the different results obtained may rely on different animal species used, and different doses and times assayed.

Four hours after APAP administration, HSP70 appeared in urine. To our knowledge, this is the first report that studies the appearance of HSP70 in urine from APAP-intoxicated animals. The fact that no hepatic induction of HSP70 occurs after APAP administration suggests the renal origin of HSP70, at least in the experimental conditions of the present study. HSP70 and NAG appeared in urine earlier than creatinine and urea are significantly increased in blood. Urinary HSP70 and NAG excretion occurred at the same time as the kidney showed signs of histological damage. Forty-eight hours after APAP administration, HSP70 is still induced in the cortical homogenates, no histological damage is demonstrated, and HSP70 is not detected in urine. As suggested by Mueller et al. [26] the loss of tubular integrity would be an important factor that results in the appearance of HSP70 in the urine.

Heat shock protein functions at the cellular level to protect cells against a wide variety of acute stress conditions [39]. It has been suggested that HSP inducers would represent a new antidote to APAP-induced hepatotoxicity [40]. Based on our present results, we suggest that HSP inducers might be assayed as potential therapeutic agents against APAP-induced nephrotoxicity. HSP70 induction, combined with the extent of renal damage, could be monitored by its urinary excretion and by urinary NAG excretion.

Acknowledgements We thank Wiener Laboratories, Rosario, Argentina for the gift of analytical reagents. This work was supported by the following grant: SECYT-UNR Nº. 459/2007 (to LT).

References

1. Boyer TD, Rouff SL (1971) Acetaminophen-induced hepatic necrosis and renal failure. JAMA 218:440–441
2. Cobden I, Record CO, Ward MK, Kerr DN (1982) Paracetamol-induced acute renal failure in the absence of fulminant liver damage. Br Med J (Clin Res Ed) 284:21–22
3. Mour G, Feinfeld DA, Caraccio T, McGuigan M (2005) Acute renal dysfunction in acetaminophen poisoning. Ren Fail 27: 381–383
4. Mitchell JR, McMurtry RJ, Statham CN, Nelson SD (1977) Molecular basis for several drug-induced nephropathies. Am J Med 62:518–526
5. McMurtry RJ, Snodgrass WR, Mitchell JR (1978) Renal necrosis, glutathione depletion, and covalent binding after acetaminophen. Toxicol Appl Pharmacol 46:87–100
6. Newton JF, Bailie MB, Hook JB (1983) Acetaminophen nephrotoxicity in the rat. Renal metabolic activation in vitro. Toxicol Appl Pharmacol 70:433–444
7. Emeigh Hart SG, Beierschmitt WP, Bartolone JB, Wyand DS, Khairallah EA, Cohen SD (1991) Evidence against deacetylation and for cytochrome p450-mediated activation in acetaminophen-induced nephrotoxicity in the cd-1 mouse. Toxicol Appl Pharmacol 107:1–15
8. Eguia L, Materson BJ (1997) Acetaminophen-related acute renal failure without fulminant liver failure. Pharmacotherapy 17: 363–370
9. Trumper L, Girardi G, Elias MM (1992) Acetaminophen nephrotoxicity in male wistar rats. Arch Toxicol 66:107–111
10. Trumper L, Coux G, Monasterolo LA, Molinas S, Garcia VM, Elias MM (2005) Effect of acetaminophen on the membrane anchoring of Na+, K+ATPase of rat renal cortical cells. Biochim Biophys Acta 1740:332–339
11. Molitoris BA, Dahl R, Geerdes A (1992) Cytoskeleton disruption and apical redistribution of proximal tubule Na+, K+ATPase during ischemia. Am J Physiol 263:F488–F495
12. Van Why SK, Kim S, Geibel J, Seebach FA, Kashgarian M, Siegel NJ (1999) Thresholds for cellular disruption and activation of the stress response in renal epithelia. Am J Physiol 277:F227–F234
13. Aufricht C, Bidmon B, Ruffingshofer D, Regele H, Herkner K, Siegel NJ, Kashgarian M, Van Why SK (2002) Ischemic conditioning prevents Na+, K+ATPase dissociation from the cytoskeletal cellular fraction after repeat renal ischemia in rats. Pediatr Res 51:722–727
14. Aufricht C (2005) Heat-shock protein 70: molecular supertool? Pediatr Nephrol 20:707–713
15. Borkan SC, Gullans SR (2002) Molecular chaperones in the kidney. Annu Rev Physiol 64:503–527
16. Wakui H, Komatsuda A, Miura AB (1995) Heat-shock proteins in animal models for acute renal failure. Ren Fail 17:641–649
17. Donati YR, Slosman DO, Polla BS (1990) Oxidative injury and the heat shock response. Biochem Pharmacol 40:2571–2577
18. Schober A, Muller E, Thurau K, Beck FX (1997) The response of heat shock proteins 25 and 72 to ischaemia in different kidney zones. Pflugers Arch 434:292–299
19. Van Why SK, Hildebrandt F, Ardito T, Mann AS, Siegel NJ, Kashgarian M (1992) Induction and intracellular localization of HSP-72 after renal ischemia. Am J Physiol 263:F769–F775
20. Cowley BD, Gudapaty S (1995) Temporal alterations in regional gene expression after nephrotoxic renal injury. J Lab Clin Med 125:187–199
21. Komatsuda A, Wakui H, Satoh K, Yasuda T, Imai H, Nakamoto Y, Miura AB, Itoh H, Tashima Y (1993) Altered localization of 73-kilodalton heat-shock protein in rat kidneys with gentamicin-induced acute tubular injury. Lab Invest 68:687–695
22. Chen Q, Yu K, Stevens JL (1992) Regulation of the cellular stress response by reactive electrophiles. The role of covalent binding and cellular thiols in transcriptional activation of the 70-kilodalton heat shock protein gene by nephrotoxic cysteine conjugates. J Biol Chem 267:24322–24327
23. Beck FX, Neuhofer W, Muller E (2000) Molecular chaperones in the kidney: distribution, putative roles, and regulation. Am J Physiol Renal Physiol 279:F203–F215
24. Aufricht C, Lu E, Thulin G, Kashgarian M, Siegel NJ, Van Why SK (1998) ATP releases HSP-72 from protein aggregates after renal ischemia. Am J Physiol 274:F268–F274
25. Bidmon B, Endemann M, Muller T, Arbeiter K, Herkner K, Aufricht C (2000) Heat shock protein-70 repairs proximal tubule structure after renal ischemia. Kidney Int 58:2400–2407
26. Mueller T, Bidmon B, Pichler P, Arbeiter K, Ruffingshofer D, VanWhy SK, Aufricht C (2003) Urinary heat shock protein-72 excretion in clinical and experimental renal ischemia. Pediatr Nephrol 18:97–99
27. Mitchell JR, Jollow DJ, Potter WZ, Davis DC, Gillette JR, Brodie BB (1973) Acetaminophen-induced hepatic necrosis. I. Role of drug metabolism. J Pharmacol Exp Ther 187:185–194
28. Mugford CA, Tarloff JB (1997) The contribution of oxidation and deacetylation to acetaminophen nephrotoxicity in female Sprague-Dawley rats. Toxicol Lett 93:15–22
29. Trumper L, Monasterolo LA, Elias MM (1996) Nephrotoxicity of acetaminophen in male Wistar rats: role of hepatically derived metabolites. J Pharmacol Exp Ther 279:548–554
30. Ellman GL (1959) Tissue sulfhydryl groups. Arch Biochem Biophys 82:70–77
31. Laemmli UK (1970) Cleavage of structural proteins during the assembly of the head of bacteriophage t4. Nature 227:680–685
32. Hosseini R, Dehpour AR, Rad MH, Rankohi K (1997) An improved method for evaluation of nephrotoxicity by assay of urinary N-acetyl β-d-glucosaminidase (NAG) activity. Toxicol Mech Methods 7:153–176
33. Sedmak JJ, Grossberg SE (1977) A rapid, sensitive, and versatile assay for protein using Coomassie brilliant blue G250. Anal Biochem 79:544–552
34. Salminen WF Jr, Voellmy R, Roberts SM (1997) Differential heat shock protein induction by acetaminophen and a nonhepatotoxic regioisomer, 3′-hydroxyacetanilide, in mouse liver. J Pharmacol Exp Ther 282:1533–1540
35. Sumioka I, Matsura T, Kai M, Yamada K (2004) Potential roles of hepatic heat shock protein 25 and 70i in protection of mice against acetaminophen-induced liver injury. Life Sci 74:2551–2561
36. Prescott LF (1983) Paracetamol overdosage. Pharmacological considerations and clinical management. Drugs 25:290–314

37. Hoivik DJ, Fisher RL, Brendel K, Gandolfi AJ, Khairallah EA, Cohen SD (1996) Protein arylation precedes acetaminophen toxicity in a dynamic organ slice culture of mouse kidney. Fundam Appl Toxicol 34:99–104
38. Salminen WF Jr, Voellmy R, Roberts SM (1998) Effect of n-acetylcysteine on heat shock protein induction by acetaminophen in mouse liver. J Pharmacol Exp Ther 286:519–524
39. Westerheide SD, Morimoto RI (2005) Heat shock response modulators as therapeutic tools for diseases of protein conformation. J Biol Chem 280:33097–33100
40. Nishida T, Matsura T, Nakada J, Togawa A, Kai M, Sumioka I, Minami Y, Inagaki Y, Ishibe Y, Ito H, Ohta Y, Yamada K (2006) Geranylgeranylacetone protects against acetaminophen-induced hepatotoxicity by inducing heat shock protein 70. Toxicology 219:187–196